scientific reports

Check for updates

OPEN

An optimized shunt active power filter using the golden Jackal optimizer for power quality improvement

Derradji Bakria[1,2]✉, Abdelkader Azzeddine Laouid[1], Belkacem Korich[1], Abdelkader Beladel[1], Ali Teta[1], Ridha Djamel Mohammedi[1], Salah K. Elsayed[3], Enas Ali[4,5], Dessalegn Bitew Aeggegn[6]✉ & Sherif S. M. Ghoneim[3]

Integration of nonlinear loads in modern power systems has led to many issues arising mainly due to the generation of harmonic currents and the presence of reactive power, both having adverse effects on power quality and grid stability. Harmonic currents cause increased losses, overheating of equipment, and voltage distortions, while reactive power imbalances result in inefficiencies in power delivery and compromised system performance. To overcome these problems, a Shunt Active Power FIlter design and an optimal control strategy for harmonic mitigation and reactive power compensation are proposed in this paper. The design incorporates an optimized anti-windup PI controller for DC-link voltage regulation and an optimized output filter to enhance the quality of the injected current. This design is formulated as an optimization problem and solved using the Golden Jackal Optimizer. MATLAB/Simulink simulations validate the proposed method under different operating conditions, covering dynamic change of loads and unbalanced grid conditions. The result shows a remarkable reduction in Total Harmonic Distortion (THD) of grid current, and reactive power compensation meanwhile maintaining the stability of the grid.

Keywords Golden Jackal optimization, Shunt active power filter (SAPF), Optimal control, Power quality, Current harmonics compensation

Abbreviations
SAPF	Shunt Active Power Filter
VSI	Voltage Source Inverter
AHF	Active Harmonic Filter
SRF	Synchronous Reference Frame
PI	Proportional-Integral (Controller)
THD	Total Harmonic Distortion
GJO	Golden Jackal Optimization
PSO	Particle Swarm Optimization
GA	Genetic Algorithm
GWO	Grey Wolf Optimization
ACO	Ant Colony Optimization
V_s	Source Voltage
V_L	Load Voltage
V_{dc}	DC-Link Voltage

[1]Applied Automation and Industrial Diagnostics Laboratory LAADI, Ziane Achour University of Djelfa, PO Box 3117, Djelfa 17000, Algeria. [2]Department of Electrical Engineering, LASER Lab, Ziane Achour University of Djelfa, PO Box 3117, Djelfa 17000, Algeria. [3]Department of Electrical Engineering, College of Engineering, Taif University, Taif 21944, Saudi Arabia. [4]Centre for Research Impact & Outcome, Chitkara University Institute of Engineering and Technology, Chitkara University, Rajpura 140401, Punjab, India. [5]Faculty of Engineering and Technology, Future University in Egypt, New Cairo 11835, Egypt. [6]Department of Electrical and Computer Engineering, Debre Markos University, Debre Markos, 269, Debre Markos, Ethiopia. ✉email: derradji.bakria@univ-djelfa.dz; dessalegn_bitew@dmu.edu.et

I_s	Source Current
I_F	Filter Current
L_f	Output filter inductance
R_f	Output filter inductance

Power electronic devices account for a large proportion of industrial and residential applications, such as car battery chargers, and their high efficiency makes them not only one of the key components of but also a powerful energy conversion device. However, these devices operate as nonlinear loads that can greatly affect the quality of electrical power in transmission systems[1,2].

Reactive power plays a crucial role in maintaining a stable and efficient electrical grid. When there's not enough of it, voltage levels can fluctuate or even collapse, which can disrupt sensitive equipment and impact the entire system's stability. In contrast, excessive reactive power leads to wasted energy and higher transmission losses. It also puts extra strain on transformers and generators, causing them to overheat, wear out faster, and require more maintenance. Furthermore, reactive power can contribute to harmonic distortion, which interferes with electronic devices and reduces overall power quality[3].

In this context, the literature explains a variety of solutions for improving grid power quality and ensuring its stable operating conditions. Certainly, what has contributed most to this development is the development of controllable power electronic devices like Insulated Gate Bipolar Transistors (IGBTs) and Silicon Carbide devices (SiC) that are incorporated into sophisticated power-generation management systems. If managed properly, these systems can mitigate harmonic distortions and compensate for the reactive power caused by nonlinear loads, thus increasing the efficiency and stability of the whole power network.

The shunt active power filter is widely employed to enhance the quality of the grid. It comprises a voltage source inverter connected in parallel with the grid allowing the injection of real-time compensating currents for harmonic distortions and reactive power. Such a VSI is interfaced with the grid via a filter at its output; this smoothes the injected current. This process contributes greatly to the mitigation of the side effects of harmonic currents and offers stabilized voltage levels. Their effectiveness greatly relies on the speed and effectiveness of their algorithms, along with the design consideration of the output filters. In the system of SAPF, there exists a control unit that contains three important algorithms. The first is harmonic detection and extraction, which is classified into time-domain, frequency-domain, and combined methods[4–16]. The second algorithm is the DC-link voltage regulation algorithm, which is generally based on a PI controller in order to keep the DC link voltage at its desired value[17–19]. While the last is the current controller algorithm, it's the most important part in any SAPF system for accurate current reference tracking.

Much attention has gone to research activities aimed at proposing advanced controllers, hence ensuring maximal possible speed of approach, high precision, and the required stability of a given system. For instance, the deadbeat controller has been widely exploited due to its high precision, robustness, and fast response, but its dependence on the model of the system results in large tracking errors when it is driven to operate under suboptimal conditions[20,21]. On the other hand, the hysteresis controller is valued for its simplicity and ease of implementation but suffers from the drawback of variable switching frequency[22,23]. Moreover, the sliding mode controllers (SMC) have a high level of robustness against disturbances and system uncertainties but may suffer from stability problems in some cases[24–27]. Fuzzy Logic Control (FLC) is potent in dealing with vague and imprecise inputs, but it strongly relies on the knowledge of experts and demands updates of the rule base in many instances[26,27]. Additionally, repetitive control is featured with poor dynamic response and is thereby constrained to perform under fast-changing conditions[28,29]. The controller based on the Lyapunov function has high tracking accuracy but suffers from some drawbacks like variable switching frequency, the necessity of high sampling rates, and high computational burden[30,31]. Table 1 presents a summary of different controllers used in past works.

Generally, controller tuning and parameter design strategies are classified into three major approaches. The first one includes classical tuning methods, which involve both analytical and numerical techniques[32]. The second approach is the self-tuning methods, which are based on adaptive control principles, such as Model Reference Adaptive Control (MRAC), whereby parameters are automatically updated according to a reference model[33]. Lastly, smart tuning methods make full use of modern optimization and intelligent techniques to carry out precise and optimal adjustments in parameters. These methods dramatically improve the system performance; hence, they are the most effective solution for the difficulties posed by today's applications[1,34]. Most of the studies carried out so far indicate that most of the SAPF systems are dependent on conventional approaches, which have

Control Strategy	Strengths	Limitations	References
Deadbeat Controller	*High precision, robustness, and fast response*	*High dependence on system model; large tracking errors under suboptimal conditions*	19,20
Hysteresis Controller	*Simple implementation and fast dynamic response*	*Variable switching frequency leading to increased switching losses*	21,22
Sliding Mode Control (SMC)	*High robustness against disturbances and uncertainties*	*Potential stability issues and chattering effect*	23–26
Fuzzy Logic Control (FLC)	*Handles vague/imprecise inputs; does not require an exact model*	*Strongly relies on expert knowledge; requires frequent rule base updates*	25,26
Repetitive Control	*Effective for periodic disturbances*	*Poor dynamic response; limited performance in fast-changing conditions*	27,28
Lyapunov-based Controller	*High tracking accuracy*	*Variable switching frequency; high computational burden*	29,30

Table 1. Comparison of control strategies for SAPF systems.

Tuning Method	Characteristics	Limitations	References
Classical Tuning	*Uses analytical/numerical techniques for root placement*	*May not be efficient for modern, complex power systems*	[31]
Self-Tuning (Adaptive)	*Adjusts parameters automatically using adaptive control*	*Based on older methodologies, potentially inefficient*	[32]
Smart Tuning (Optimization)	*Uses metaheuristic techniques for precise adjustments*	*May suffer from poor balance between exploration and exploitation*	[1,33–36]

Table 2. Comparison of controller tuning and parameter design strategies.
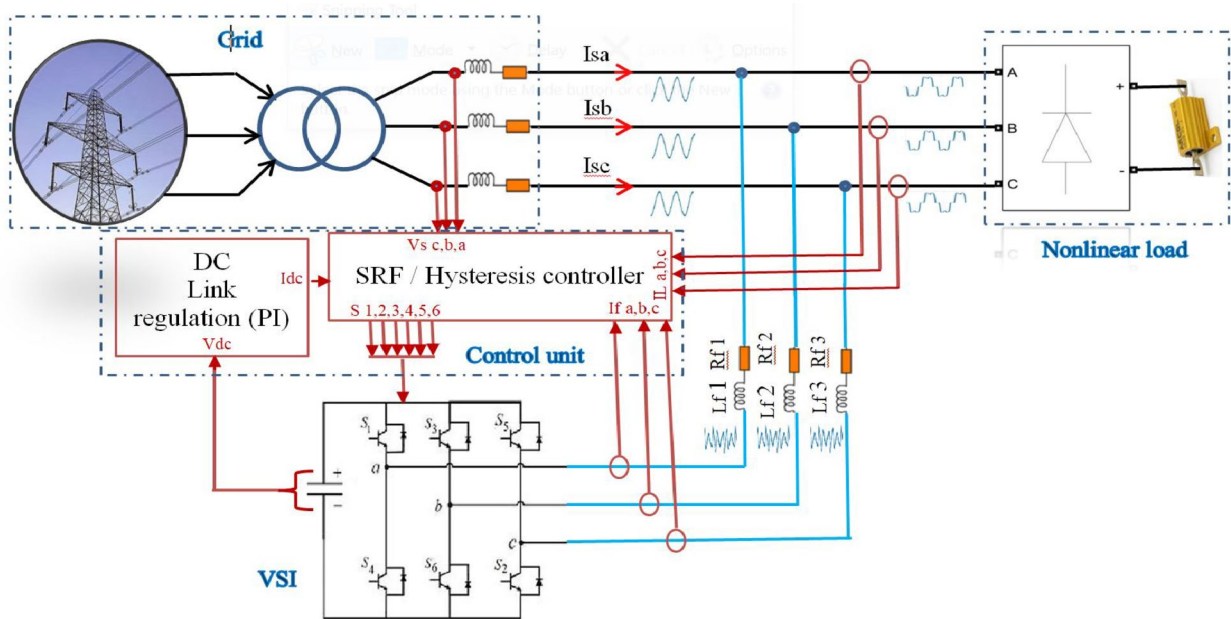
Fig. 1. System Configuration of the Three-Phase Shunt Active Power Filter.

some limitations. Consequently, this can lead to improper control adjustments, probable instability and poor performance under critical conditions.

In the wake of these limitations and developments in control and optimization, better controllers through precise design and optimal tuning are an urgent need, especially for an improvement in compensation performances. The integration of metaheuristic approaches has indeed revolutionized power quality enhancement strategies by changing the design and control approaches of the SAPFs. This integration has shown promising potential in achieving optimizations for essential factors such as proportional-integral (PI) controller gains via metaheuristic techniques[1,32,34–37]. However, most of these methods have difficulties finding a balance between exploration and exploitation, which is necessary to prevent the algorithms from falling into early convergence and not reaching global optimization. In this respect, ongoing research is developing new algorithms for such a problem. In summary, Table 2 provides an overview of the existing literature regarding the controller design and parameter tuning strategies.

Accordingly, in this paper we introduce a methodology to determine the optimal design of SAPF system with an anti-windup PI controller and a hysteresis controller for effective overall power quality improvement. This design combines a hysteresis controller within the internal current control loop, leveraging its fast response and flexibility to rapidly track current reference signals, an optimized DC link PI controller to improve the performance of the inverter, and an optimized output filter to enhance the quality of the injected current.

As pointed before, one of the main difficulties in SAPF design is the tuning of control parameter, which has a significant influence on system performance. Thus, our design relies on the Golden Jackal Optimizer (GJO) to obtain the PI controller and output filter optimal parameters. The GJO achieves a good balance between exploration and exploitation during optimization and avoids local optima to maximize overall system efficiency. The objective function is formulated in a way that it compromises on reducing harmonic distortion, improves the dynamic response, and maximizes power quality. Simulation studies confirm that the new method effectively suppresses harmonic intrusions in the grid current and effective reactive power compensation compared to conventional tuning methods.

System description

The configuration scheme of the three-phase SAPF system is represented in Fig. 1. This SAPF is connected between the grid and the harmonic-generating nonlinear load to mitigate all harmonic-generated power quality issues. The main parts contained in this system are:
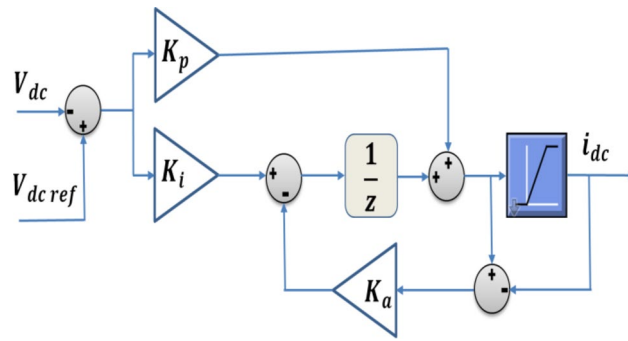
Fig. 2. PI controller with windup handling.
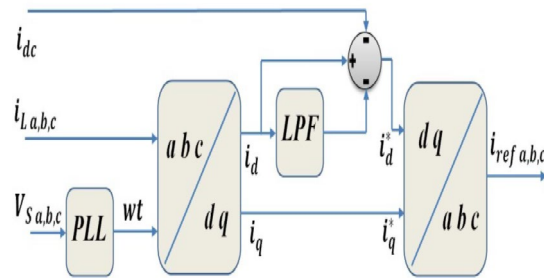
Fig. 3. Reference Current Extraction Using the SRF.

- **DC link capacitor**.

Added to the DC side of the inverter is a capacitor. This is an energy storage element for providing the required energy for harmonic compensation. It is a very critical component and plays a very important role in order to maintain a stable DC-link voltage and to keep the inverter operational.

- **Voltage Source Inverter (VSI)**.

VSI is the heart of the SAPF. The VSI converts the DC energy from the capacitor into AC currents opposing the harmonic and reactive components in the grid. VSI operates on the basis of PWM techniques for precise compensation.

- **Output filter**.

Inductors are connected between the VSI and the grid. They are the transmission elements which smooth the output currents of the inverter and provide a good synchronization with the grid. Moreover, they operate as filters to damp the high-frequency noise produced during the switching process.

- **Control Unit**.

The control unit performs real-time monitoring and control of the SAPF. It uses advanced algorithms in the detection of harmonic distortions, among other power quality issues on the grid. The control system produces accurate reference signals for the VSI to inject compensating currents effectively. Most modern applications use either instantaneous reactive power theory or synchronous reference frame methods for better performance, which ensures reliable operation under dynamic conditions.

Control unit description

The control unit constitutes the heart of the three-phase SAPF. The essence of the operating principle of this control unit includes real-time control and monitoring, so that one can effectively have harmonic mitigation that ensures improvement of power quality. It consists of three sections: harmonic extraction, DC-link voltage regulation, and current control.

In this study, we selected a PI controller for DC-link voltage regulation, the Synchronous Reference Frame (SRF) method for harmonic extraction[14,37,38], and a hysteresis controller for the current control loop. The schematics of these sections are presented in Figs. 2 and 3, and 4, respectively.
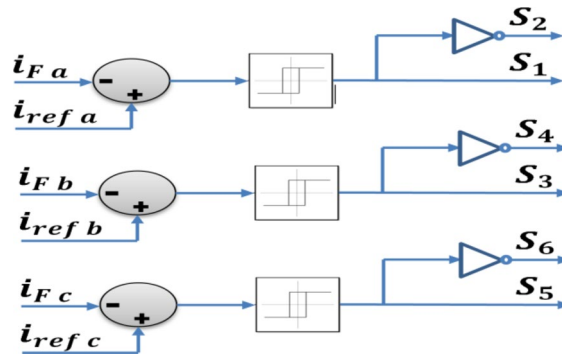
Fig. 4. Hysteresis current controller.

Optimal design of the PI controller and RL output filter
The PI controller parameters (K_p, K_i, and K_a) are tuned to achieve rapid response and minimal steady-state error. Similarly, the RL output filter is designed to reduce interactions between the inverter and the grid, ensuring stable operation and efficient harmonic compensation. The optimization process considers system dynamics and power quality standards.

Optimization problem formulation
The optimization process aims at improving the performance of the three-phase SAPF by minimizing three key factors: the DC-link voltage error, the current error, and the Total Harmonic Distortion (THD) of the grid currents. These factors are combined into one fitness function that will be used for the evaluation of the system performance.

The fitness function is defined as the weighted sum of the three components:

$$F = w_1 \times E_{DC} + w_2 \times E_I + w_3 \times THD \tag{1}$$

IAE will be the performance index that will be used to judge the deviations of both DC-link voltage and current errors over time. It gives the accumulated absolute error to ensure a comprehensive evaluation of system stability and dynamic response.

$$E_{DC} = \int_{t-T}^{t} |V_{dc\,ref} - V_{dc}| \tag{2}$$

$$E_I = \int_{t-T}^{t} |i_{ref} - i_F| \tag{3}$$

Golden Jackal optimizer
The GJO is a new nature-inspired metaheuristic proposed by Chopra and Ansari to solve optimization problems; it is inspired from the social and hunting behaviors of golden jackals. GJO has been developed on the basis of building balanced exploration and exploitation between the male and female jackals in the search space. This optimizer is more suited for finding the solutions to complex engineering optimization problems[39].

This algorithm utilizes the two most important agents, namely, the male jackal and the female jackal, which are the best and the second-best solutions, respectively. Dynamic positions of these two jackals are used to drive the population of the search agents toward the optimal solutions. Taking inspiration from the evading behavior of the jackals, an energy factor E is introduced that can be dynamically updated depending on the number of iterations. Depending on the factor, either the exploration or exploitation of the algorithm will be considered. Another novelty introduces the algorithm by means of the distribution of Levy flights to improve exploration by randomizing step size. The flow chart of the GJO is represented in Fig. 5 as summary of its steps.

The movement of the jackals in the search space can be modeled by the following equations:

$$\vec{X}(t+1) = \vec{X}_P - E \times \vec{D} \tag{4}$$

$$\vec{D}_1 = \left| \vec{X}_P - \vec{R}_L \times \vec{X}(t) \right| \tag{5}$$

$$\vec{D}_2 = \left| \vec{R}_L \times \vec{X}_P - \vec{X}(t) \right| \tag{6}$$

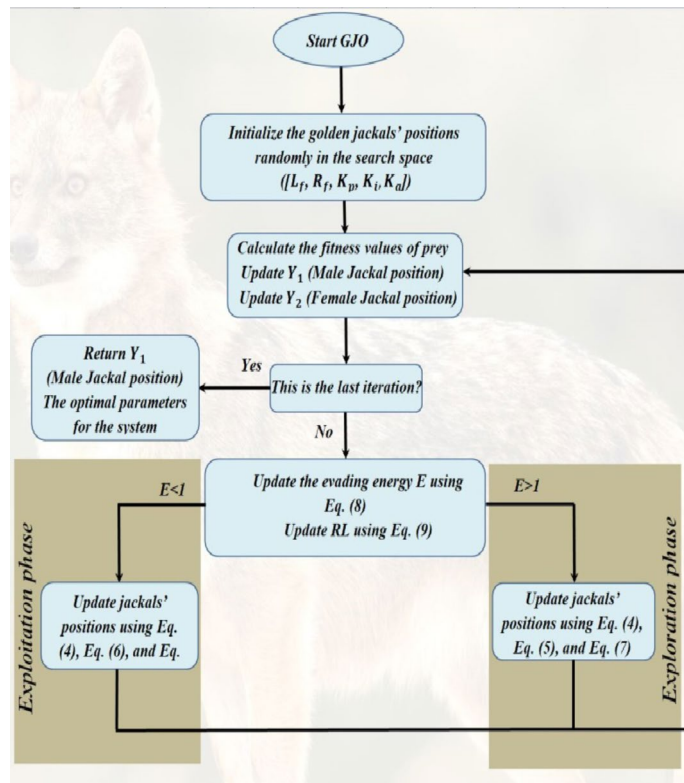$$\vec{X}_{new} = \frac{\vec{X}(t+1)_{male} + \vec{X}(t+1)_{female}}{2} \tag{7}$$

With.

Fig. 5. Flow chart of GJO.

$\overrightarrow{X}(t)$ is the current position of the jackal.

$\overrightarrow{X}(t+1)$ is the new position according to the position female or the male jackal.

$\overrightarrow{X}_P$ is the position of the male and female jackals.

$\underrightarrow{E}$ is the evading energy.

$\underrightarrow{D}$ is the distance between the current position and the prey.

$\overrightarrow{R}_L$ is a random factor derived from Levy flight distribution.

$$E = \left(1.5 \times \frac{1.5 \times iteration}{Max\ iteration} \right) \times (2 \times r_1 - 1) \tag{8}$$

$$\overrightarrow{R}_L = 0.05 \times levy \tag{9}$$

Where.

r_1 is a random number between 0 and 1.

$iteration$ is the current iteration.

$Max\ iteration$ is the maximum iteration number.

$levy$ is a random factor derived from Levy flight distribution.

The update mechanism is divided into two phases based on $|E|$. When $|E| > 1$ (exploration phase), search agents update their positions relative to the male and female jackals using Eqs. (4), (5), and (7). Conversely, when $|E| < 1$ (exploitation phase), the position updates are governed by Eqs. (4), (6), and (7).

Results and discussion

A sophisticated simulation was developed using the MATLAB/Simulink programming environment to thoroughly investigate the dynamic response and behavior of the SAPF when exposed to an assortment of rigorous usage profiles. The tests put the SAPF through a series of demanding situations, such as rapidly changing loads producing transient load currents, unbalanced source voltage levels, and dramatically fluctuating reactive power demands.

GJO evaluation against PSO, GWO, and ACO

The performance of the GJO was compared with three well-known optimizers: Particles Swarm Optimizer (PSO), Grey Wolf Optimizer (GWO), and Sine Cosine Algorithm (SCA), based on their convergence behavior. The optimization parameters for each algorithm are given in Table 3.

Figure 6 shows the convergence curves of the algorithms, from which the superiority of GJO can be clearly observed. The GJO has a fast convergence rate in the initial iterations and keeps a stable upward trend toward the

Description	GJO	GWO	PSO	SCA
Population size	20			
Maximum number of iterations	50			
Number of decision variables	5			
Search agents	$[L_f, R_f, K_p, K_i, K_a]$			
Lower bound	[0.5 mH, 0.3Ω, 0.001, 0.1, 0.01]			
Upper bound	[5 mH, 20Ω, 10, 100, 100]			
The objective function	Equation (1)			
Weights	1			
Load	Load 3			

Table 3. Parameters of the optimization.
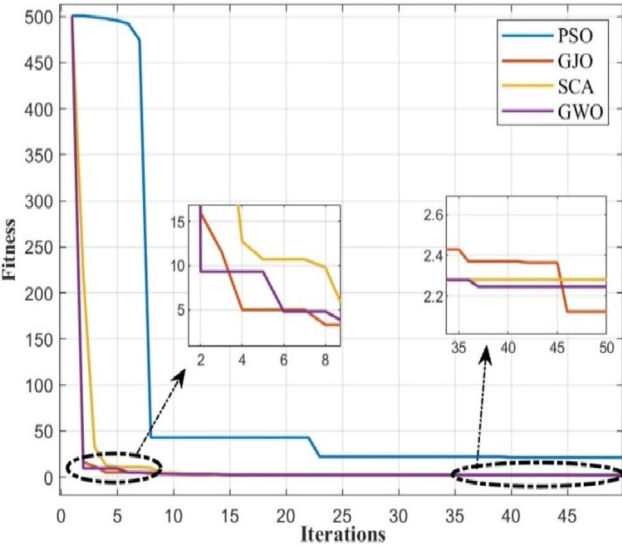
Fig. 6. Convergence curves.

Parameters	GJO	GWO	SCA	PSO
L_f	0.0023	0.002	0.0024	0.0015
R_f	0.34	0.36	0.34	0.38
K_p	0.066	0.13	0.1146	12.7
K_i	0.79	5.77	1.02	61.38
K_a	20	6	2	5.62
Fitness	2.12	2.25	2.28	21.26

Table 4. Optimization results.

global optimum. This means that the algorithm has a very good balance between exploration and exploitation, enabling it to outperform PSO, GWO, and SCA in terms of better avoidance of local optima for more optimal solutions. Further, the following Table 4 presents the obtained fitness values and the parameters optimized by each method.

Optimized SAPF evaluation

The performance of the designed Shunt Active Power Filter (SAPF) was evaluated using simulation parameters detailed in Table 5, with Load 3 as the test condition. The SAPF was activated at $t = 0.2s$, and the results are illustrated in Fig. 7, which contains five subplots describing key aspects of the system's operation.

Figure 7-a presents the DC link voltage and its reference, demonstrating that the optimized controller effectively tracks the reference voltage with no overshoot and achieves a settling time of just $0.35\,s$. This reflects the controller's precision and stability in regulating the DC link voltage. Figure 7-b shows the grid voltage, where

Description	Value
Grid voltage	$70\sqrt{3}V$
DC-link capacitor	*2200 μF*
Sampling time	$10^{-6}s$
Load 1	*Three phase rectifier + 10Ω*
Load 2	*Three phase rectifier + 10Ω + 100 μF*
Load 3	*Three phase rectifier + 10Ω + 1 100 μF + three phase RL load $R = 1\Omega$, $L = 20\ mH$*

Table 5. Parameters of the system.

a minor voltage drop is observed after the SAPF is connected, and indicating minimal impact on grid voltage stability.

Figure 7-c illustrates the currents of the grid, load, and SAPF. The optimized system successfully generates the required compensation current to eliminate harmonics and reactive power, resulting in a sinusoidal grid current. This is further validated in Fig. 7-d, which provides an FFT analysis of the grid current (i_{sa}), showing a significant reduction in Total Harmonic Distortion (THD) from 14.64% to 0.8%. Additionally, the magnitude of the current was reduced from $23.9\ A$ to $15.71\ A$, demonstrating the SAPF's effectiveness in improving current quality.

Finally, Fig. 7-e presents the reactive power analysis of the grid and the load. Before SAPF activation, the reactive power from the grid was approximately $2000\ VAR$. After activation, the SAPF successfully compensated for the reactive power, reducing it to nearly zero, thereby ensuring optimal power factor correction.

The next evaluation is to compare the performance of the proposed SAPF with the results presented in[1]. According to Fig. 8b which represent the FFT analysis of the grid current captured from[1], the optimized proportional-resonant (PR) controller, designed using the Genetic Algorithm (GA), achieved a Total Harmonic Distortion (THD) of 3.86%. In contrast, as shown in Fig. 8.a the proposed SAPF, utilizing the optimized controller, achieved a significantly lower THD of 0.86%. The test was conducted under the same load and grid conditions as described in[1], which are detailed in Table 5 of our paper, where the load corresponds to load 1. Additionally, a comparison of the DC link voltage performance reveals that the proposed controller demonstrates superior regulation characteristics.

Specifically, the overshoot of the proposed controller is only 6 V, whereas the controller in[1] exhibits a significantly higher overshoot of 12 V.

The final evaluation of the proposed SAPF was conducted under unbalanced grid voltage conditions, where the voltage V_{sc} was reduced by 20%. Initially, the system was tested with Load 1 under the unbalanced grid, and at $t = 1\ s$, the load was switched to Load 2. Despite this dynamic and challenging scenario, the optimized SAPF demonstrated its robustness and effectiveness by significantly reducing the THD and compensating for reactive power.

The results, illustrated in Fig. 9, confirm the SAPF's excellent performance. Figure 9-a shows the DC link voltage and its reference, where the SAPF successfully maintains stability and tracks the reference throughout the load transition. Figure 9-b shows the grid voltage under the unbalanced condition in which the system keeps working effectively though the voltage goes down. Figure 9-c illustrates grid, load, and SAPF currents the results confirm also that although the voltage is unbalanced and the dynamic load change also occurs, SAPF can maintain the sinusoidal grid current. Figure 9-d shows the FFT analysis of grid current, which is showing a significant reduction in THD. Figure 9-e shows the reactive power compensation result, and here, the SAPF is able to reduce the reactive power to nearly zero in the grid.

Conclusion

This paper presented an optimization approach for the PI controller and the output filter in a Shunt Active Power Filter (SAPF) system. The design of both the controller and the filter was formulated as an optimization problem, which was then solved using the Golden Jackal Optimizer (GJO). GJO has been selected after comparing its convergence performance with the convergence performance of three well-known optimizers, namely Grey Wolf Optimizer, Sine Cosine Algorithm, and Particle Swarm Optimization. The outcome of this comparison proved that GJO had superior convergence performance and is the best suitable optimizer for the said application.

The optimized SAPF system has been tested under nominal grid conditions, unbalanced grid, and dynamic load variations. Tests yielded much better results in THD reduction, harmonic elimination, and reactive power compensation. The optimized PI controller ensured that the DC link voltage was regulated in a fast and stable way, while the optimized output filter minimized grid distortion by improving the quality of the injected current. Both enhancements are critical in maintaining the overall performance and reliability of the SAPF system. Moreover, the extended comparative analysis with the state-of-the-art studies confirmed that the proposed optimization approach outperforms the existing methods, especially regarding THD reduction, DC link voltage overshoot, and overall system stability.

In conclusion, the main contributions of this paper are as follows:

- Development of an optimized PI anti-windup regulator for DC link voltage regulation.
- Optimization of the output filter in SAPF systems to enhance the quality of the injected current.
- Comprehensive evaluation of the proposed method under normal, unbalanced, and dynamic load scenarios.
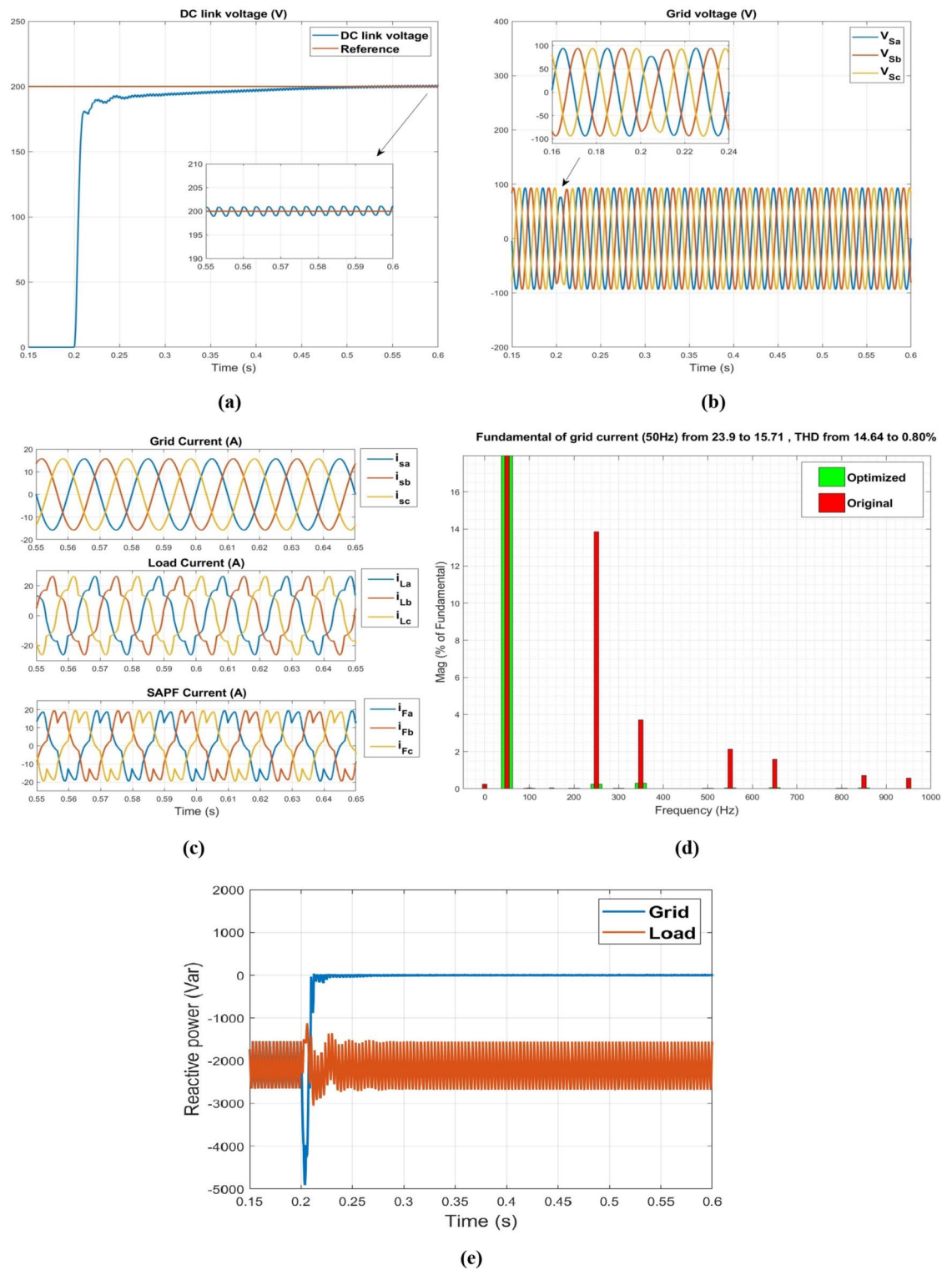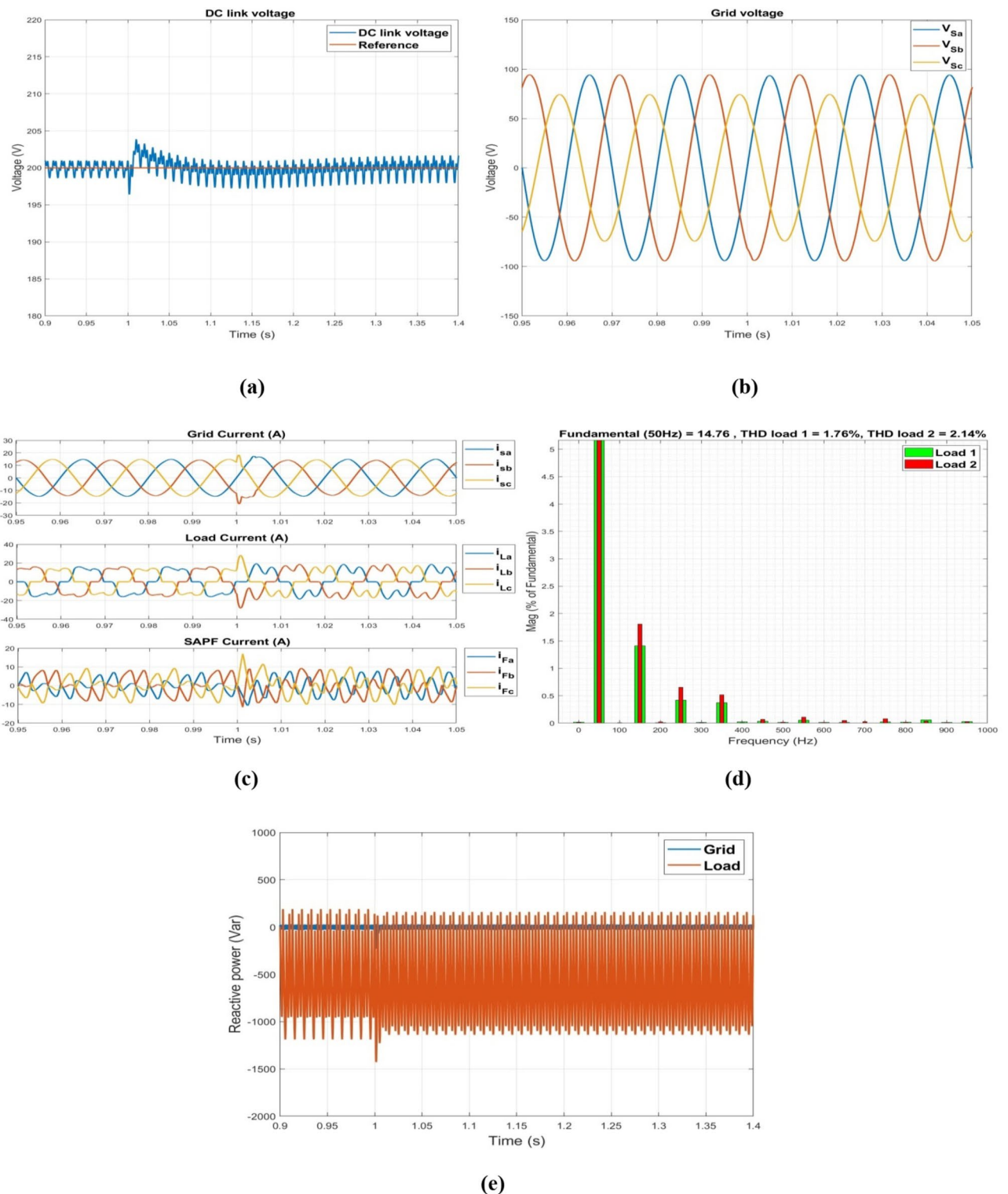
Fig. 7. Performance of the optimized SAPF system with load 3 under balanced grid conditions.

- A comparative analysis with recent works, demonstrating superior performance in harmonic compensation and dynamic response.
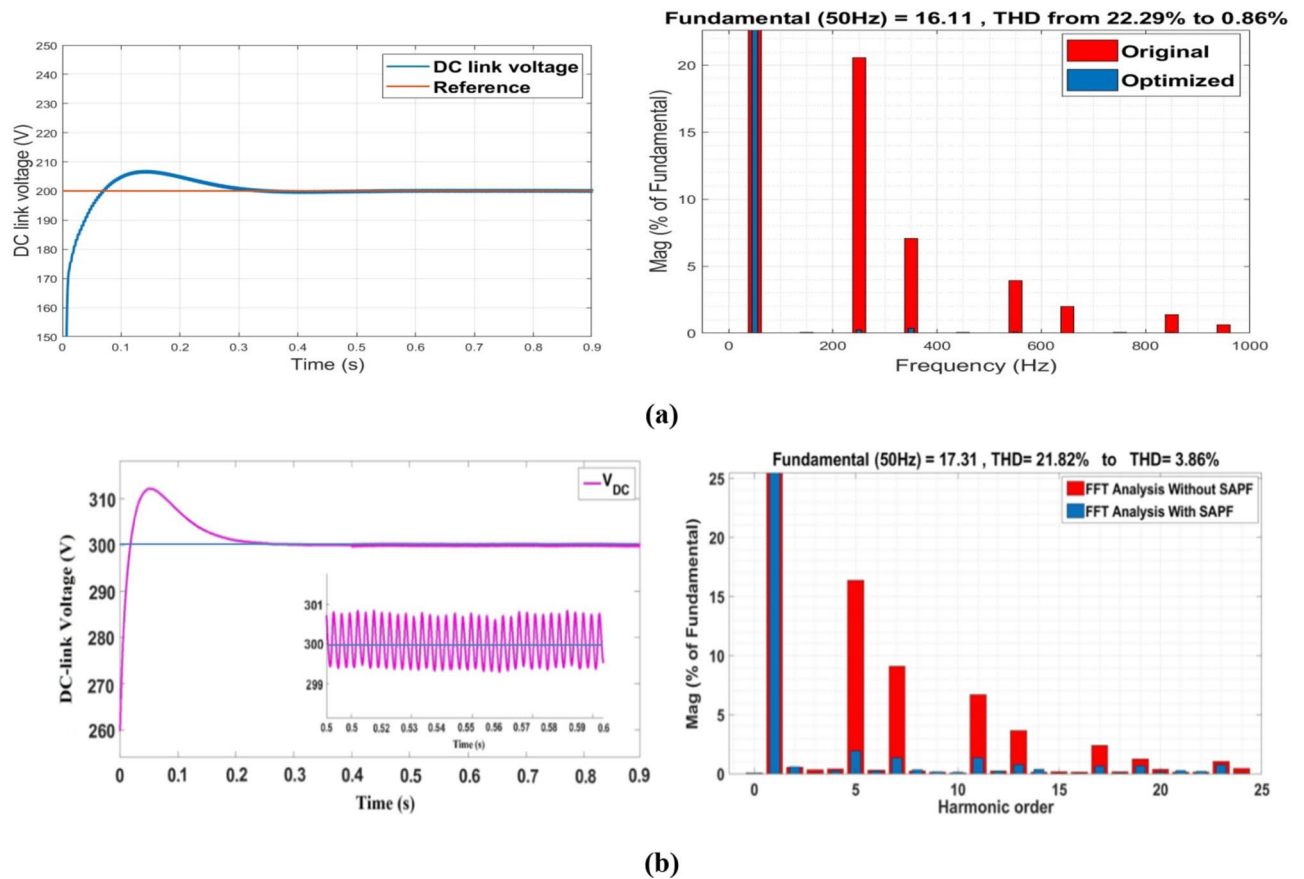
Fig. 8. Comparison between the optimized SAPF system and the system in[1]: (a) Performance of the optimized SAPF with load 1 under balanced grid conditions, (b) Results from[1].

(a)

(b)

(c)

(d)

(e)

Fig. 9. Performance of the optimized SAPF with dynamic load and unbalanced grid voltage.

Data availability

References

1. Amini, B., Rastegar, H. & Pichan, M. An optimized proportional resonant current controller based genetic algorithm for enhancing shunt active power filter performance. *Int. J. Electr. Power Energy Syst.* **156**, 109738 (2024).
2. Bighash, E. Z., Sadeghzadeh, S. M., Ebrahimzadeh, E. & Blaabjerg, F. Adaptive-harmonic compensation in residential distribution grid by roof-top PV systems. *IEEE J. Emerg. Sel. Top. Power Electron.* **6** (4), 2098–2108 (2018).
3. Tabatabaei, N. M., Aghbolaghi, A. J., Bizon, N. & Blaabjerg, F. (eds) *Reactive Power Control in AC Power Systems* Vol. 1 (Springer International Publishing, 2017).
4. Ferrari, M. Evaluation of harmonic detection algorithms for active power filter based on voltage and current detection methods. In *2018 9th IEEE International Symposium on Power Electronics for Distributed Generation Systems (PEDG)* (pp. 1–8). IEEE. (2018), June.
5. Chen, D., Xiao, L., Yan, W., Li, Y. & Guo, Y. A harmonics detection method based on triangle orthogonal principle for shunt active power filter. *Energy Rep.* **7**, 98–104 (2021).
6. Han, Y. et al. Study on a novel approach to active power filter control using neural network-based harmonic identification scheme. *Electr. Eng.* **91**, 313–325 (2010).
7. Abed, A. M., El-Sehiemy, R. A., Touati, B. B. & Arwash, E. H. M. Accurate Identification of Harmonic Distortion for Micro-Grids using Artificial Intelligence-Based Predictive Models. *IEEE Access.* (2024).
8. Eskandarian, N., Beromi, Y. A. & Farhangi, S. Improvement of dynamic behavior of shunt active power filter using fuzzy instantaneous power theory. *J. Power Electron.* **14** (6), 1303–1313 (2014).
9. Tsvetanov, D., Djagarov, N., Grozdev, Z. & Djagarova, J. Synchronous reference frame theory control for current harmonics suppression in ship power system using shunt active power filter. In *2022 International Conference Automatics and Informatics (ICAI)* (pp. 120–128). IEEE. (2022), October.
10. Guo, Z. et al. An impedance identification-based islanding detection method for droop control inverters based on RDFT and positive–negative Notch filters. *Energy Rep.* **8**, 1060–1070 (2022).
11. Sundaram, E. & Venugopal, M. On design and implementation of three phase three level shunt active power filter for harmonic reduction using synchronous reference frame theory. *Int. J. Electr. Power Energy Syst.* **81**, 40–47 (2016).
12. Büyük, M., İnci, M., Tan, A. & Tümay, M. Improved instantaneous power theory based current harmonic extraction for unbalanced electrical grid conditions. *Electr. Power Syst. Res.* **177**, 106014 (2019).
13. Kumar, S. S., Arya, K., Chandrakala, K. V. & Nadar, K. P. Implementation of Instantaneous PQ Theory to Improve Power Quality by Shunt Active Power Filter for Non-Linear Loads. In *2024 IEEE 3rd International Conference on Electrical Power and Energy Systems (ICEPES)* (pp. 1–6). IEEE. (2024), June.
14. Pandey, A. & Singh, A. SWRDFT controller for single phase grid tied PV system with low voltage ride through capability. *Electr. Power Syst. Res.* **214**, 108878 (2023).
15. Baros, J. et al. Review of fundamental active current extraction techniques for SAPF. *Sensors* **22** (20), 7985 (2022).
16. Han, C., Xinyan, Y., Pengfei, J., Bingyuan, Y. & Ke, D. Dynamic optimization for shunt active power filter to selectively extract harmonics with Vector Discrete Fourier Transform. In *2023 IEEE 14th International Symposium on Power Electronics for Distributed Generation Systems (PEDG)* (pp. 971–977). IEEE. (2023), June.
17. Li, Z., Ren, M., Chen, Z., Liu, G. & Feng, D. A bi-sliding mode PI control of DC-link voltage of three-phase three-wire shunt active power filter. *IEEE J. Emerg. Sel. Top. Power Electron.* **10** (6), 7581–7588 (2022).
18. Fallah, M., Modarresi, J., Kojabadi, H. M., Chang, L. & Guerrero, J. M. A modified indirect extraction method for a single-phase shunt active power filter with smaller DC-link capacitor size. *Sustain. Energy Technol. Assess.* **45**, 101039 (2021).
19. Musarrat, M. N., Islam, M. R., Muttaqi, K. M. & Sutanto, D. Shunt active DC filter to reduce the DC-link ripple current caused by power converters to improve the lifetime of aluminum electrolytic capacitors. *IEEE Trans. Ind. Appl.* **57** (4), 4306–4315 (2021).
20. Pichan, M., Seyyedhosseini, M. & Hafezi, H. A new DeadBeat-based direct power control of shunt active power filter with digital implementation delay compensation. *IEEE Access.* **10**, 72866–72878 (2022).
21. Pariz, P. & Monfared, M. A deadbeat controller design for single-phase active power filters based on forward-backward discretization. In *2021 12th Power Electronics, Drive Systems, and Technologies Conference (PEDSTC)* (pp. 1–5). IEEE. (2021), February.
22. Singh, J. K. & Behera, R. K. An improved hysteresis current controller for grid-connected inverter system to address power quality issues at reduced switching frequency. *IEEE Trans. Ind. Appl.* **57** (2), 1892–1901 (2021).
23. Raghutu, R., Manoj, V. & Yegireddy, N. K. Shunt Active Power Filter with Three Level Inverter using Hysteresis Current Controllers. In *E3S Web of Conferences* (Vol. 540, p. 06001). EDP Sciences. (2024).
24. Li, Y. et al. A sliding mode SVPWM method for a HTS shunt active power filter. *IEEE Trans. Appl. Supercond.* **31** (8), 1–2 (2021).
25. Choudhury, S., Acharya, D. P., Sahu, S. K., Khan, A. & Dash, T. Robust Sliding Mode Controller and Shunt Active Power Filter for Improvement of Power Quality Indices of an Autonomous Microgrid. In *Machine Vision and Augmented Intelligence: Select Proceedings of MAI 2022* (pp. 345–356). Singapore: Springer Nature Singapore. (2023).
26. Fei, J., Wang, Z. & Pan, Q. Self-constructing fuzzy neural fractional-order sliding mode control of active power filter. *IEEE Trans. Neural Networks Learn. Syst.* **34** (12), 10600–10611 (2022).
27. Patel, P. et al. Adaptive Controller With Fuzzy and Modified SRF-Based SAPF for Harmonics Reduction Under Distorted Source Conditions. In *2024 IEEE 13th International Conference on Communication Systems and Network Technologies (CSNT)* (pp. 1–7). IEEE. (2024), April.
28. Nazir, R. et al. Advanced digital repetitive control of shunt active power filter. *Electr. Eng.* **105** (4), 2217–2228 (2023).
29. Guo, X., Lin, H. & Chen, G. SiC-MOSFET shunt active power filter based on half-cycle SDFT and repetitive control. *Energy Rep.* **7**, 246–252 (2021).
30. Çelik, D. Lyapunov based harmonic compensation and charging with three phase shunt active power filter in electrical vehicle applications. *Int. J. Electr. Power Energy Syst.* **136**, 107564 (2022).
31. Bajaj, M. et al. A lyapunov-function based controller for 3-phase shunt active power filter and performance assessment considering different system scenarios. *IEEE Access.* **9**, 66079–66102 (2021).
32. Patel, R., Samal, P., Panda, A. K. & Guerrero, J. M. Implementation of bio-inspired flower pollination algorithm in distribution system harmonic mitigation scheme. In *2021 1st International Conference on Power Electronics and Energy (ICPEE)* (pp. 1–7). IEEE. (2021), January.
33. Ray, P. K. & Swain, S. D. Performance enhancement of shunt active power filter with the application of an adaptive controller. *IET Generation Transmission Distribution.* **14** (20), 4444–4451 (2020).
34. Boudechiche, G. et al. Anti-windup FOPID-based DPC for SAPF interconnected to a PV system tuned using PSO algorithm. *Eur. J. Electr. Eng.* **22** (4–5), 313–324 (2020).
35. Mishra, A. K. et al. PSO-GWO optimized fractional order PID based hybrid shunt active power filter for power quality improvements. *IEEE Access.* **8**, 74497–74512 (2020).
36. Sao, J. K., Naayagi, R. T., Panda, G., Patidar, R. D. & Swain, S. D. SAPF parameter optimization with the application of Taguchi SNR method. *Electronics* **11** (3), 348 (2022).
37. Duc, M. L., Hlavaty, L., Bilik, P. & Martinek, R. Harmonic mitigation using meta-heuristic optimization for shunt adaptive power filters: A review. *Energies* **16** (10), 3998 (2023).
38. Barva, A. V. Analysis of SAPF based on pq and SRF theory for different supply and load conditions. In *2023 International Conference on Power, Instrumentation, Energy and Control (PIECON)* (pp. 1–6). IEEE. (2023), February.

39. Chopra, N. & Ansari, M. M. Golden Jackal optimization: A novel nature-inspired optimizer for engineering applications. *Expert Syst. Appl.* **198**, 116924 (2022).

Author contributions
Derradji Bakria, Abdelkader Azzeddine Laouid, Belkacem Korich, Abdelkader Beladel, Ali Teta, Ridha Djamel Mohammedi: Conceptualization, Methodology, Software, Visualization, Investigation, Writing- Original draft preparation. Salah K. Elsayed, Enas Ali, Dessalegn Bitew Aeggegn, Sherif S.M. Ghoneim: Data curation, Validation, Supervision, Resources, Writing - Review & Editing, Project administration, Funding Acquisition.

Declarations

Competing interests
The authors declare no competing interests.

Conflict of interest
Authors stated that no conflict of Interest.

Additional information
Correspondence and requests for materials should be addressed to D.B. or D.B.A.

Reprints and permissions information is available at www.nature.com/reprints.

Publisher's note Springer Nature remains neutral with regard to jurisdictional claims in published maps and institutional affiliations.